Design of Interfering Mobile Device in the Band Wi-Fi with Magnetron

Jan LEUCHTER, Huy DONG QUANG

Department of Radar Technology, Faculty of Military Technology,
University of Defence, Kounicova 156/65, 662 10 Brno, Czech Republic

jan.leuchter@unob.cz, quanghuy.dong@unob.cz

DOI: 10.15598/aeee.v16i4.2438

Abstract. *The aim of this article is to design an interfering mobile device with a magnetron for the interference in Wi-Fi signal in the band 2.4–2.5 GHz. Propulsion of the interfering mobile device will be implemented using system of the stepper motor, which will be controlled with the help of the microcontroller ATmega 16. In order to deal with the interfering part, it is necessary to design an inverter 12 V/4000 V and 50–60 Hz. The inverter is a supply of the high-powered vacuum tube that generates microwaves; magnetron. Magnetron is used as a source of electromagnetic interference high-frequency acting on targets, which operates in the band of Wi-Fi signal. For example, waves of high-frequency radio damage on-board electronic devices of the UAV, and by the way, we can disable fly of UAV in demarcated areas. The interfering mobile device will be used as a preparation interference and measurement electromagnetic compatibility of electronic military equipment.*

Keywords

Interfering, inverter, microcontroller, stepper motor, wi-fi signal.

1. Introduction

The mobile device can drive forward, backward, turn left, turn right and change velocity of the device. Rotation of the antenna positioned in the mobile device is controlled in space 0–180° due to the wiring of an interfering part. Mobile interfering device is implemented by four stepper motors to drive propulsion of the mobile device. It also has a fifth stepper motor, which is placed on top of the mobile device and is used to rotate the antenna of the interfering part with a magnetron (0–180°). In this article, a test version of the interfering mobile device will be presented (see Fig. 1).

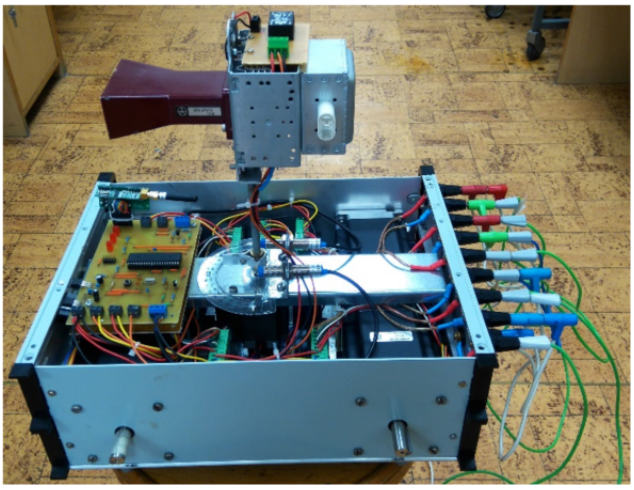

Fig. 1: A test version of the mobile device.

The model consists of seven main parts. The first part is "propulsion of the device" containing five motors that provide force to drive the mobile device and rotate the antenna. For this application in this article, we chose four hybrid bipolar stepper motors SX34-2970 [10] for driving the mobile device and one hybrid bipolar stepper motor LDO-57STH76-2804 [12] for the rotation of the antenna. The second part is "power" which provides DC voltage for all parts of the mobile device. For the test version, this part will be the power supply Agilent E3633. The third part is "driver" that provides a rated current to the motor's windings in the shortest possible time. The fourth part is "block control" which controls the overall functionality of the interfering mobile device. As far as "block control" is concerned, this part includes the microcontroller ATmega 16. The fifth part is "remote control" that will be made by the sub-miniature transmitter module MTX2

and the universal receiver module MRX1 from company Flajzar [13]. The sixth part is "limit rotation of the antenna" that will be implemented with the help of the two inductive proximity sensors LJ12A3-4-Z/BY. The two sensors allow to set an initial location of the antenna to 90° and limit rotation of the antenna in the 0–180° sector. The seventh part is "block noise" including an interfering circuit with the magnetron. On the test version, the "block noise" will be not used with magnetron, but a sign of the active interference sequence will be indicated by the LED placed on top of the mobile device.

2. Conception of the Mobile Device

2.1. Propulsion of the Mobile Device

1) Why the Stepper Motor?

The propulsion of the mobile device can be implemented using the servo motor or the stepper motor. Selecting between a servo motor and a stepper motor can be quite a challenge involving the balancing of several design factors. Cost considerations, torque, speed, acceleration, and drive circuity play a role in selecting the best motor for the application.

Our interfering mobile device will be used as a preparation interference of electronic military equipment. The rotation of the antenna will be limited in the 0–180° sector. According to these requirements, the propulsion of the mobile device must have sufficient torque to move in the field and flexibility in movement, e.g. move forward, backward, left, right, and change the speed of the mobile device. And according to the requirement of the antenna, the motor used must be able to accurately set their location.

Stepper motors and servo motors differ in two key aspects which are their basic construction and how they are controlled. Servo motors often require a position encoder to keep track of the position of the motor shaft, especially if precise movements are required. A system like this operates through a closed-loop feedback. The difference between the desired position and the measured position is used to compute the direction and magnitude of a drive applied to the motor. Such system is best achieved by applying control theory, otherwise, the results can be poor, oscillatory or even catastrophic. Driving a stepper motor to a precise position is much simpler than driving a servo motor. Stepper motors with digital control allow to set precise positions without position encoder and closed-loop feedback. The torque of the stepper motor at low speed is greater than the servo motor of the same size. The motor has full torque in the rest position (when current is applied on the coil). Stepper motors have a high reliability because the engine does not contain any of the contact brushes [9].

Nevertheless, stepper motors have several limitations. They are more difficult to control at very high speeds, and often permanently draw current in applications even when the motor is not rotated. With these qualities, stepper motor is selected for the implementation of the propulsion of the mobile device.

2) Basic Principle of Stepper Motor

A stepper motor is a brushless DC synchronous electric motor that divides a full rotation into a number of equal steps. The motor's position can then be commanded to move and hold at one of these steps without any feedback sensor (an open-loop controller), as long as the motor is carefully sized to the application in respect of torque and speed [9] and [11].

The stepper is composed of a stator and a rotor as most electric motors (see Fig. 2). Stator contains several pairs of coils (often four pairs) that can be variously connected (two and two coils connected one side of the winding, all the coils with a common one side, in series, parallel, etc.). The rotor is a roller made of magnetically soft or hard material with salient poles. There are three main types of stepper motor [9], but in this article, only one of them will be shown, namely a hybrid synchronous stepper motor (see Fig. 2).

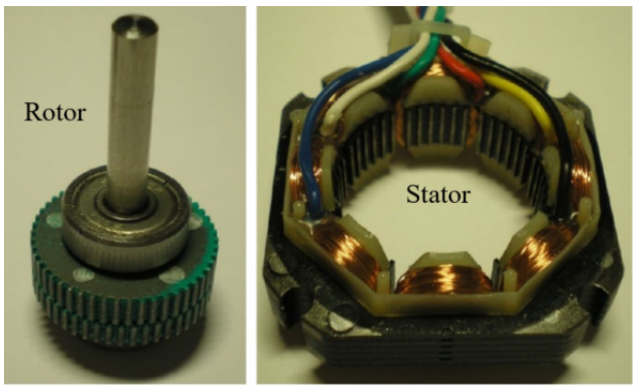

Fig. 2: Construction of hybrid stepper motor.

The basic principle of the hybrid synchronous stepper motor is simple. The current passing through the coil of the stator creates a magnetic field which attracts the opposite pole of the rotor [9]. By using a suitable connection of the coils, we made a magnetic field that rotates the rotor. According to the required torque, accuracy as setting position, and the allowable consumption, we chose any of the variants of the controls.

3) Stepper Motor Driver Circuits

There are two basic winding arrangements for the electromagnetic coils in the hybrid stepper motor, which are unipolar and bipolar stepper motor. Both types differ in the method of control. Unipolar drivers always energize the phases in the same way and can be implemented with simple transistor circuitry. The disadvantage is that there is less available torque because the only haft of the coils can be energized at a time. Excitation of bipolar stepper motor needs H-bridge circuity to reverse the current flow through the phases [11], [4] and [5]. By energizing the phases with alternating the polarity, all the coils can be put to work by turning the motor (see Fig. 3). In this article, control of the hybrid bipolar stepper motor will be described only because both of stepper motors used belong to the hybrid bipolar stepper motor.

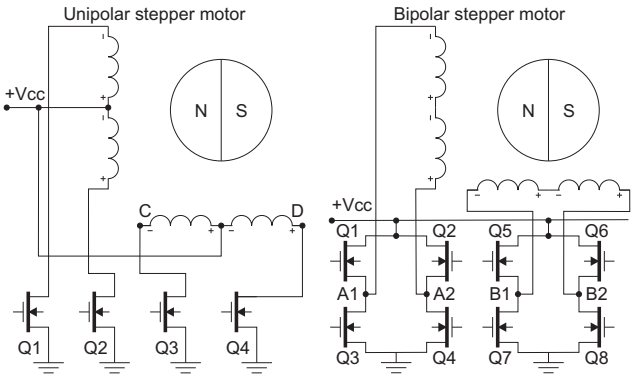

Fig. 3: Diagram of control unipolar and bipolar stepper motor [11].

Bipolar stepper motors can be controlled by one or two phases. With the single-phase control, voltage is brought only on one motor's winding. With the two-phase control, two adjacent windings are driven with an equally oriented magnetic field at the same time [11], [4] and [5]. Both methods achieve the same number of steps. But the two-phase control needs large current and will produce more torque. In this article, the two-phase control will be used for the application. Both methods belong to controlling with full step. In the full step operation, the motor moves through its basic step angle, e.g. the stepper motors used in this work have 200 steps while the step angle is 1.8°. We use the full step operation, thus for one revolution motor rotates exactly 200 steps and angle resolution is 1.8°.

The output stage of the typical two-phase bipolar drive is further illustrated in the electrical schematic diagram (see Fig. 3) and stepping sequence in Tab. 1. As illustrated, switching simply reverses the current flow through the winding thereby changing the polarity of that phase.

Tab. 1: Step sequence for bipolar two-phase control with full step [11].

Sequence	Q1–Q4	Q6–Q7	Q2–Q3	Q5–Q8
1	ON	OFF	OFF	ON
2	ON	ON	OFF	OFF
3	OFF	ON	ON	OFF
4	OFF	OFF	ON	ON

Repeating this sequence causes the rotor to rotate clockwise in 1.8° steps. From this sequence, the progress of the phase currents - A1, A2, B1, B2 - can be drawn (see Fig. 4).

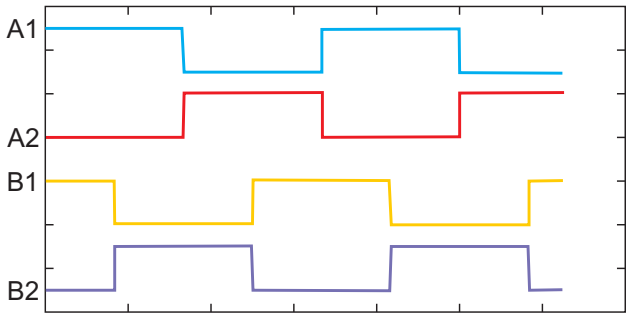

Fig. 4: The progress of the phase currents in the bipolar two-phases control with full step and clockwise.

In practice, to control a stepper motor, it is necessary to have a driver circuit. The stepper motor will need to be coupled to a driver that provides a physical electrical current to make them move. Stepper motor performance is strongly dependent on the driver circuit. Construction and principle of the driver circuit depend on the principle of control of stepper motor aforementioned. In this application, we need five drivers for controlling five stepper motors. There are several types of drivers for the hybrid bipolar stepper motor. In terms of price and features, driver DIV268N-HY-5A was selected.

Driver DIV268N-HY-5A is a two-phase hybrid stepper driver with new chip THB-6600 (see Fig. 5). The device is intended for motor with a maximum rated

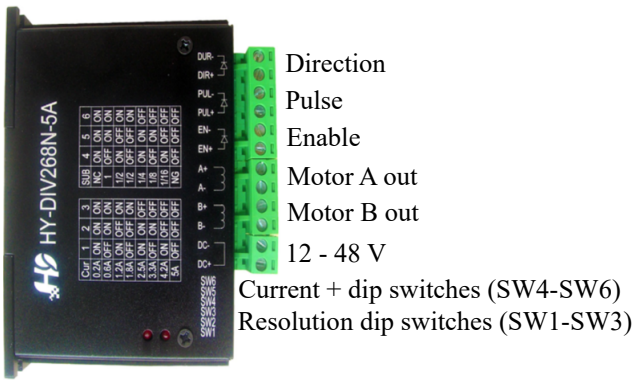

Fig. 5: Driver circuit DIV268N-HY-5A.

current of 5 A. The supply voltage may be in the range of 12–48 V.

Pins "Direction", "Pulse", and "Enable" are coupled to the microcontroller ATmega 16 for controlling direction, speed and activity of the rotation of the stepper motor. Pins "Motor A out" and "Motor B out" will be coupled to the stepper motor. Switches SW1–SW3 are used for microstepping of the stepper motor. Switches SW4–SW6 are designed to adjust the output current of the driver.

The measurement of the signals on the pin out "Motor A out" and "Motor B out" will be shown next when the motor rotates clockwise.

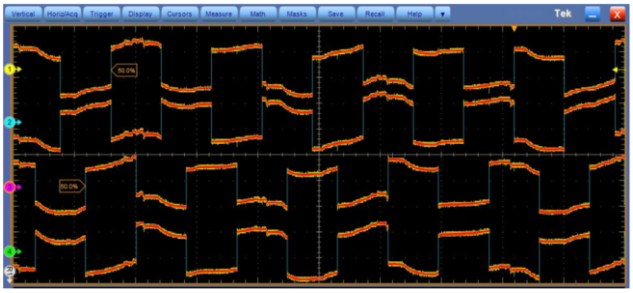

Fig. 6: The progress of the phase signals on the pin out A and B.

Progress of the phase signals on the pin out A and B of the driver are identical with those of the phase currents in the bipolar two-phase control with the full step and clockwise. Hence, this driver DIV268N-HY-5A is suitable for controlling the two-phase bipolar stepper motor.

2.2. Remote Control

As the control of the propulsion of the mobile device mentioned, the remote control is selected after deliberation, which is constructed of a serial produced module of the MTX2-SMA Transmitter micromodule with a battery holder and MRX1-SMA Receiver micromodule.

Micromodules MTX2-SMA and MRX1-SMA with the range up to several hundred meters (with reliability to 800 meters in a free space practically verified). Only the change in status is transmitted to the receiver, thereby maintaining a long battery life. Transmitter and receiver work in the range of the frequency of 868.35 MHz with an FSK modulation. Micromodules themselves have protocol for the remote communication, hence for application in this article we do not need to make any protocol communication [13].

Module transmitter was implemented on a board with 6 buttons that are connected directly to the corresponding inputs of the MTX2-SMA transmitter (see Fig. 7). Micromodule MRX1-SMA will be integrated into the part "block control". Both modules will use directional antennas 868.35 MHz.

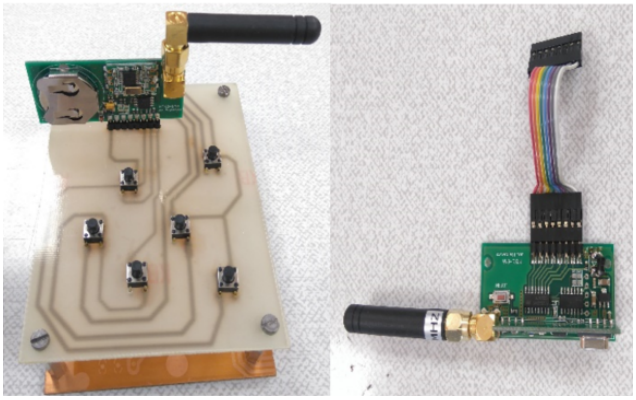

Fig. 7: Module transmitter and receiver.

The measurement of the real radiation of the module transmitter will be shown next.

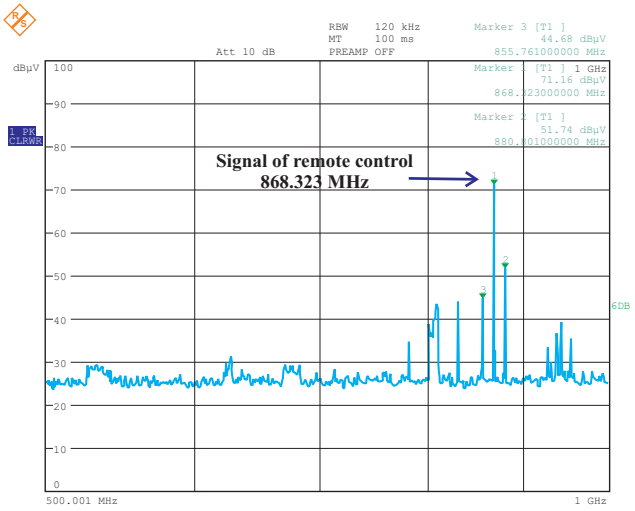

Fig. 8: The real radiation of the module transmitter.

From the graph, the higher amplitude is about 71.16 dBµV in the frequency of 868.321 MHz, and some other lower amplitudes in the frequency of 880.8 MHz and 855.76 MHz. Therefore, the main radiation of the module transmitter is in the frequency of 868.321 MHz.

2.3. Limit Rotation of the Antenna

As the principle of stepper motors mentioned above, the stepper motors are DC motors that move in discrete steps. They have multiple coils that are organized in groups called "phases". By energizing each phase in sequence, the motor will rotate, one step at a time. With a suitable algorithm of controlling the stepping, we can achieve a very precise position and speed control without feedback sensors. For controlling position, if the driver circuit and bipolar two-phase

control with the full step are used, one pulse from the microcontroller will rotate stepper motors about one step. Stepper motors used in this article have one step of about 1.8°.

A stepper motor can limit its rotation by itself. In this case, rotation in the 0–180° sector will be implemented using 100 pulses from the microcontroller. The next requirement is to set an initial position for the antenna. The initial position has a vertical direction of the body of the mobile device, which is, in this case, a 90° angle from the position of 0° of the 0–180° sector horizontally. In practice, problems will occur and affect the determination of the initial position of the antenna, which is the unwanted movement of the antenna under external factors as the stepper motor is at rest and is not energized. An unwanted impact on the antenna, e.g. during transport or replacement of elements, will make the antenna rotate in unknown angle. Then, when the mobile device operates, it will not be able to accurately determine the initial position as well as the limit 0–180° sector of the antenna. This problem will be solved using two inductive proximity sensors LJ12A3-4-Z/BY (see Fig. 9).

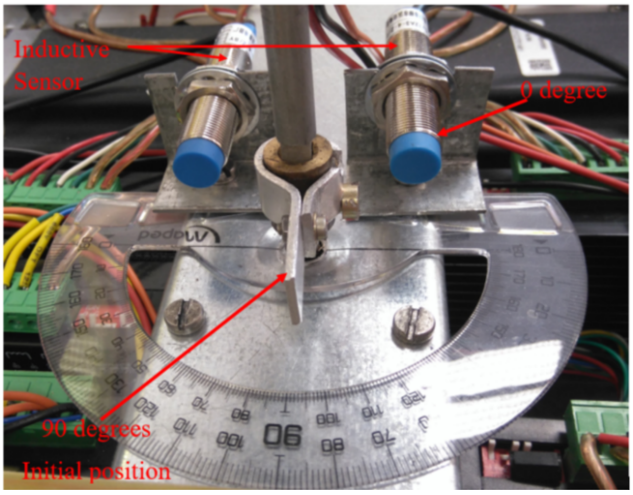

Fig. 9: Principle limit rotation of the antenna.

An inductive proximity sensor is a component widely used in the automatic control industry for detecting, controlling, and noncontact switching. When proximity switch is close to an antenna, it will send out a control signal to a microcontroller, and then the microcontroller will send a signal to a driver circuit to stop rotation of the antenna. The sensors are also used as a mechanical barrier for the antenna in case of unwanted movements. The left sensor will be used as 0° for the limited 0–180° sector (see Fig. 9).

2.4. Block Control

The main element of the block control is the microcontroller ATmega 16. In this work, the practical control with ATmega 16 will be carried out for a test version of the interfering mobile device. The block control includes input terminal for module receiver MRX1-SMA and output terminal for sending controlling signal to the driver circuit and "block noise" (see Fig. 10).

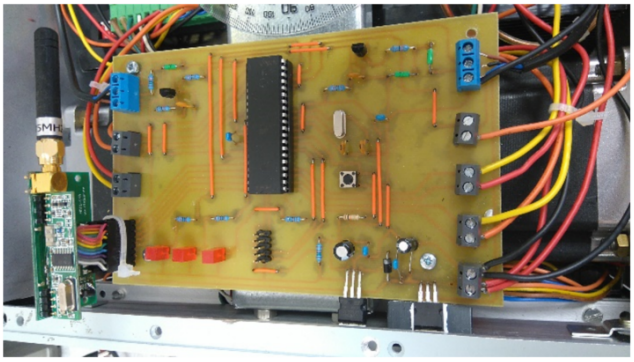

Fig. 10: Board of the block control.

The block control is possible at any time to connect to the programmer using the ISP interface and can be reprogrammed with any new algorithm or existing algorithm.

Next, Fig. 11 shows the block diagram of the digital control of the mobile device. The block control receives controlled signals from the module transmitter MTX2-SMA, and then by using a suitable algorithm, it commands the other parts of the mobile device.

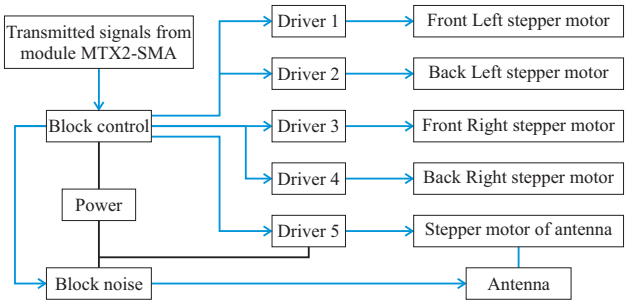

Fig. 11: Block diagram of the control mobile device.

Stepper motors on each side of the mobile device (left, right) will be controlled simultaneously. The front left and back left stepper motor will always be controlled by the same signal, and similarly for the right side. The stepper motor of antenna is controlled separately.

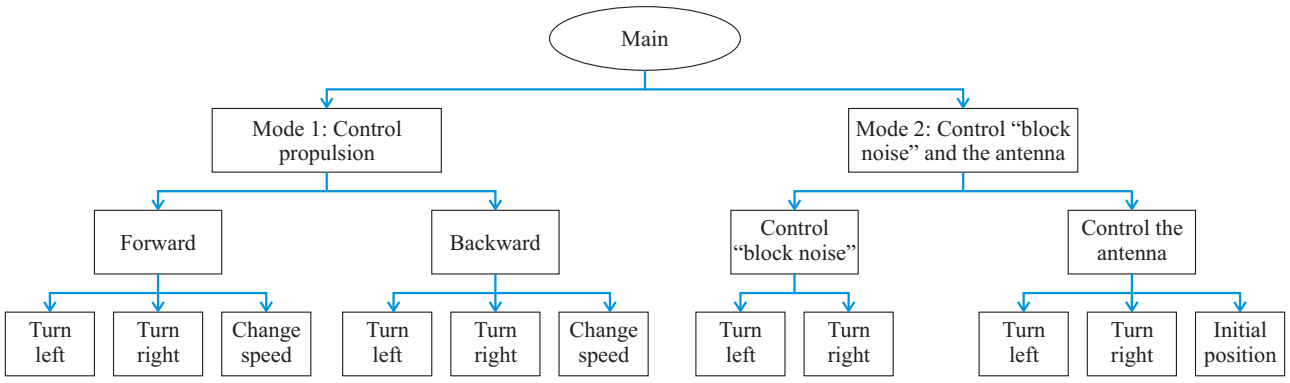

Fig. 12: The flowchart of the algorithm to control mobile device.

2.5. Algorithm to Control Mobile Device

A total algorithm to control mobile device was designed for two modes. The first mode, mode "1", is used to control the propulsion of the mobile device, e.g. driving forward, backward, and turning left, right, and changing speed. The second mode, mode "2", is designed to control the "block noise" and rotation of the antenna, e.g. on/off jammer, initial position of the antenna, limit rotation of the antenna in the 0–180° sector.

The mobile device is designed in a way that it cannot turn one of its axles. This means that turning left or right is only possible by slowing down all wheels on one side of the mobile device (turning left = slowdown in the left side, turning right = slowdown in the right side).

The algorithm is implemented in C language through Atmel Studio 7.0 development environment. The main program makes an infinite loop, which decides the active mode controls "1" or "2". Depending on the mode control, the given function is carried out by using information from the module transmitter MTX2-SMA. Figure 12 shows a flowchart of the algorithm.

3. Implementation of the Interfering Part

To deal with the interfering part of the mobile device, a magnetron was selected from microwave oven. The magnetron is used as a source of electromagnetic interference high-frequency acting on targets, which operate in the band of Wi-Fi signal [1] and [8]. To supply magnetron, it is necessary to design an inverter 12 V/4000 V and 50–60 Hz. Figure 13 shows a block diagram of the interfering part.

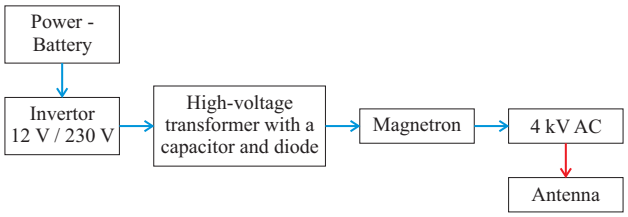

Fig. 13: Block diagram of the interfering part.

3.1. DC/AC Inverter Voltage

The main element of this part is the inverter 12 V/230 V, 50–60 Hz. High-voltage transformer and magnetron are selected from microwave oven. The antenna is pyramidal horn antenna. The design and implementation of this horn antenna will be not shown in this article.

There are many options of the design of the DC/AC inverter voltage. In term of construction and efficiency, the version push-pull forward inverter was chosen. This version is very convenient for high power application [2], [3], [6] and [7]. The diagram of the inverter is shown in Fig. 14.

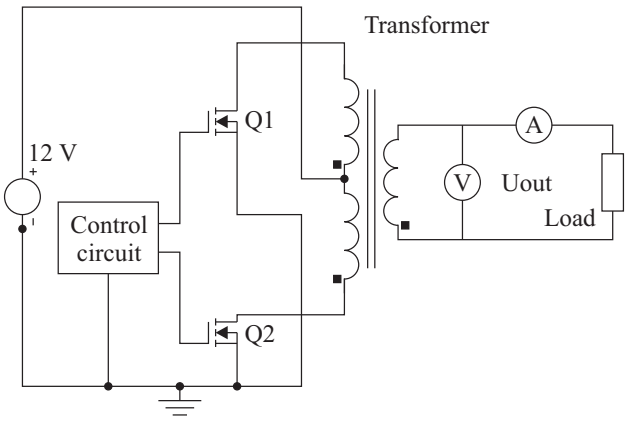

Fig. 14: Diagram of the push-pull forward inverter [6] and [7].

A basis is the control circuit equipped with two outputs specially designed for driving MOSFETs (transistors Q1, Q2) which then switch the current into the transformer and a deadtime (it basically ensures that the transistors do not engage each other, thereby reducing power consumption and increasing the efficiency of the inverter) [4] and [6].

Two outputs for driving transistors are made by the microcontroller of the "block control". But signals from microcontroller are not enough for switching MOSFETs. Hence, it is necessary to use a driver. In this application, the driver IR2101 was used. The control circuit includes the driver IR2101 and two PWM pulses. The two PWM pulses have reversed in polarity, the same 60 Hz frequency.

The ratio of the PWM signals can vary from 30 % to 70 %. The output of the transformer is connected to a voltmeter, ammeter and load of 800 Ω, 0.8 A. The result of the measurement is shown in Tab. 2.

Tab. 2: The result of the measurement of output voltage.

Ratio (%)	30	40	50	60	70
Voltage (V)	132	160	185	157	128

The output voltage achieves a maximum value 185 V in the ratio of 50 %. In Fig. 15, the waveforms of the output of the transformer (the green line) and one output of the control circuit (the yellow line) are shown.

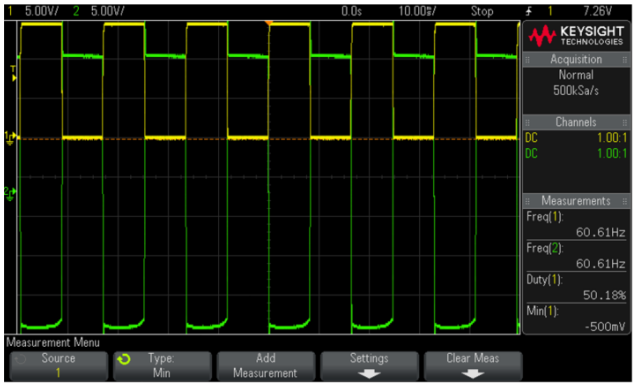

Fig. 15: The waveforms of the output signal from transformer and control circuit.

3.2. Measurement of the Magnetron

The measurement of the output of the high-voltage transformer with a diode and capacitor and measurement of the radiation of the magnetron will be shown next.

The high-voltage transformer used is transformer MOT (Microwave Oven Transformer) from a microwave oven. The difference between the MOT and normal transformer is that it has two secondary windings. The former has 3700 V with the current around of hundred mA, and the latter has 3.15–3.30 V with a current of about 10 A. Figure 16 shows a workstation for measurement of MOT and magnetron. Performance of MOT is approximately 1.5 times greater than that of the power radiated by the microwave oven.

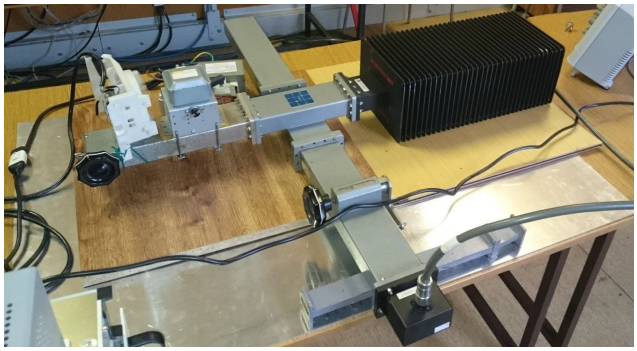

Fig. 16: The workstation for measurement MOT and magnetron.

The output voltage of the MOT was measured and displayed using a high-voltage probe. After supplying MOT, it began to generate a characteristic sound. The voltage was similar to a sinusoidal waveform with value −6.35 kV.

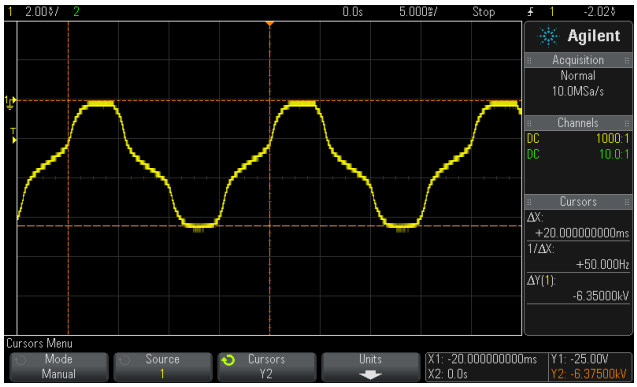

Fig. 17: Immediate output after supply MOT.

This measurement was repeated two times more for two seconds. In the first sec, signal was roughly begun to form a rectangular shape, and voltage is still negative −6.35 kV.

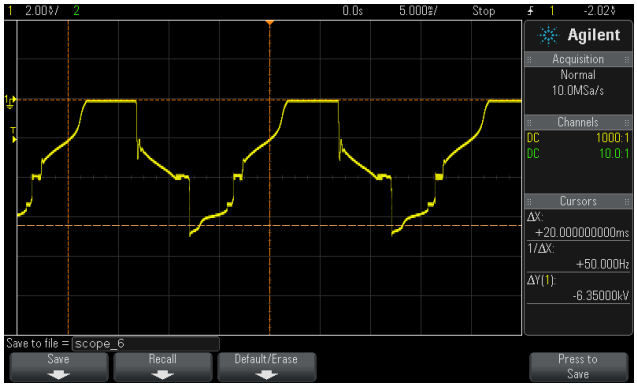

Fig. 18: Formation of the output after first second.

In the final third sec, signal already has a rectangular shape with a slight overshoot in the rising and falling edges, and voltage is −3.7375 kV.

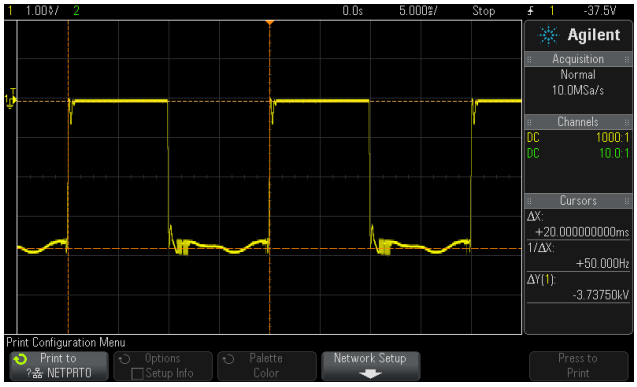

Fig. 19: Constant output after two seconds of the measurement.

The measurement of the radiation of the magnetron will be shown as follows.

Magnetron is a special kind of vacuum tube which operates as a source of microwave (high-frequency) performance with high efficiency. The generated high-frequency signal from the magnetron is dependent on dimensions of parts that comprise the magnetron.

Before measuring, it was necessary to use a power detector NBM-520 to measure the area of the entire measuring system, due to the detection of health hazardous emissions out of the system. The device measures in mW·cm^{-2}, and around the waveguides, any hazardous radiation were not measured.

Fig. 20: Measurement of the hazardous radiation.

The result of the measurement jammer is presented with the magnetron on the frequency 2.4630 GHz and its potential influence on the WIFI system (2.4395 GHz).

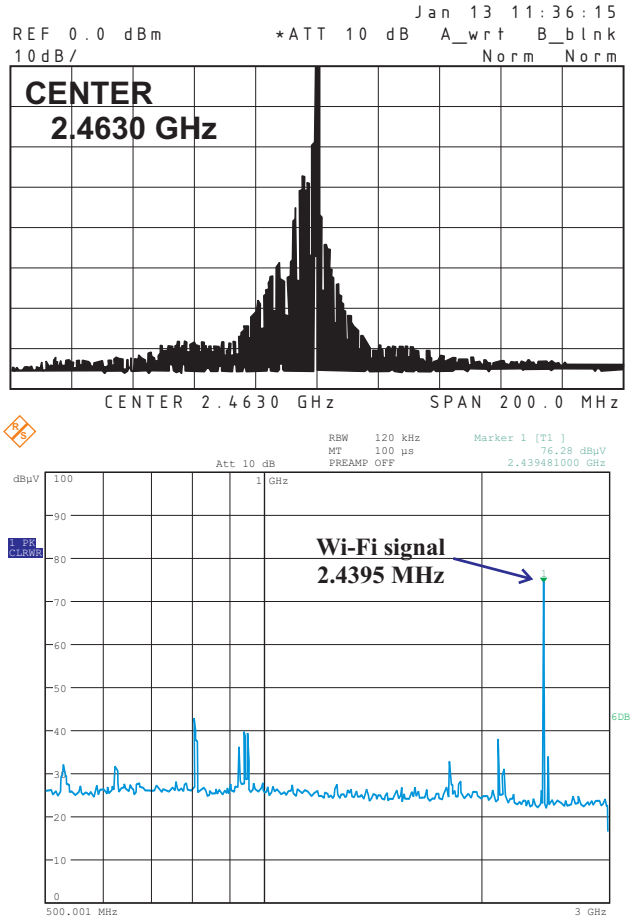

Fig. 21: Spectrum of interference with magnetron and Wi-fi signal.

4. Example of the Use of the Device

4.1. The Use of the Interfering Device

An interfering device can be used to test the susceptibility of all sensors that use the wireless signal for communication on a military field base against interference. This test allows us to take methods and increase the susceptibility of these sensors. In addition, the interfering device can be used to interfere with UAVs that would disrupt the airspace of the base.

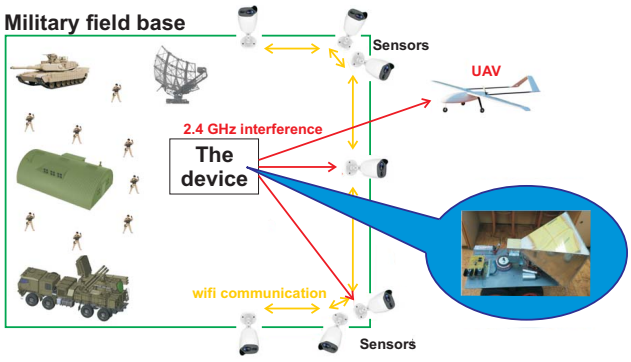

Fig. 22: Military field base.

A UAV uses 2.4 GHz - wireless to control the movement of UAV from the ground system. To limit the UAV, we can interfere with the RF signal in the 2.4 GHz frequency. The maximum power of ISM band allowed for civilian UAV is 36 dBm EIRP - 4000 mW (effective isotropic radiated power) with the maximum transmitted power of 1000 mW (30 dBm) and the minimum signal to noise ratio for the UAV is 4 dB [14] and [15]. From these parameters, we can create a system for disturbing RF signal of the UAV which has the EIRP power greater than 32 dBm, and the system operates with a frequency of 2.4 GHz [16], [17] and [18]. With these parameters, the system has the ability to interfere with and block the movement of the UAV.

For this purpose, we can use a system interfering with the magnetron which is a source of electromagnetic interference in the wireless band of 2.4 GHz with high power. The system has two main parts. The first part is a source of the transmitted power with the magnetron. The second part is an antenna system, which is used to direct the transmitted power to the desired area.

The source of electromagnetic interference can provide a transmitted power of approximately 950 W (59.3 dBm) according to the datasheet of the magnetron. The horn antenna will be used for direction of the electromagnetic interference with a gain of approximately 18 dBi. The horn antenna creates the largest group of primary emitters used in the radars and especially for very good impedance characteristics over the frequency band, the possibility to define the shape of emission characteristics and their structural simplicity [19] and [20].

The *EIRP* can be related to the power transmitted from the radio P_t, the losses (possibly including antenna mismatch) L, and the antenna gain G by [21]:

$$EIRP = P_t - L + G, \tag{1}$$

$$EIRP = 59.3 - L + 18 = 77.3 - L. \tag{2}$$

Therefore, if the designed antenna system has losses which do not reduce the EIRP below 32 dBm, the designed system can interfere UAV communication.

For this purpose, we must optimize parameters of the antenna system from the perspective of gain and losses.

Tab. 3: Calculation of parameters of the optimum horn antenna [19].

Gain	a_1 [m]	b_1 [m]	**E-plane beamwidth** (°)	**H-plane beamwidth** (°)
18	0.4346	0.3358	19.08	21.24

Here, a and b are dimensions of the horn antenna.

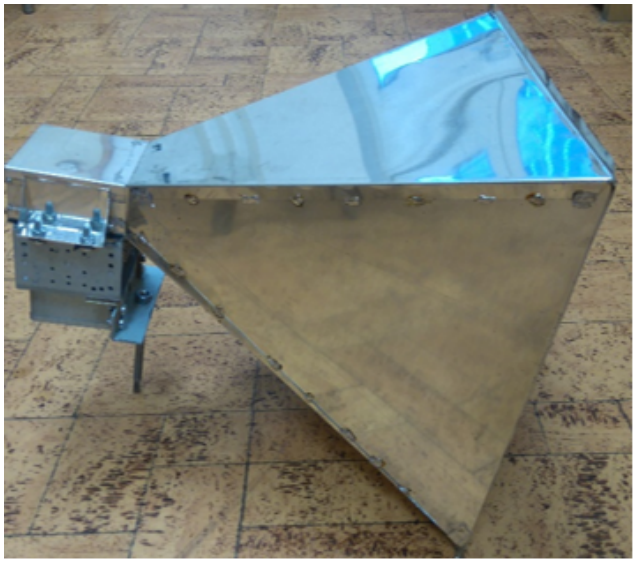

Fig. 23: The designed antenna.

Tab. 4: The results of measurement of the horn antenna in anechoic chamber.

Gain	**E-plane beamwidth** (°)	**H-plane beamwidth** (°)
18	17.6	19.7

For $G = 18$, the value of the E-plane beamwidth is smaller than that from the calculation about 1.48° and for H-plane about 1.54°.

4.2. Measurement Power of the Magnetron

Before the measurement, it is important to verify the functionality of the tested magnetron whether the cathode is not in short circuit. If everything is all correct, we can set up a measuring station.

After the power supply of the magnetron was stabilized (see Fig. 19), the voltage is −3.7375 kV and the current is 450 mA. From these results, we can calculate energy consumption.

$$P = U \cdot I \text{ (W)} = \mathbf{1681\ W}. \tag{3}$$

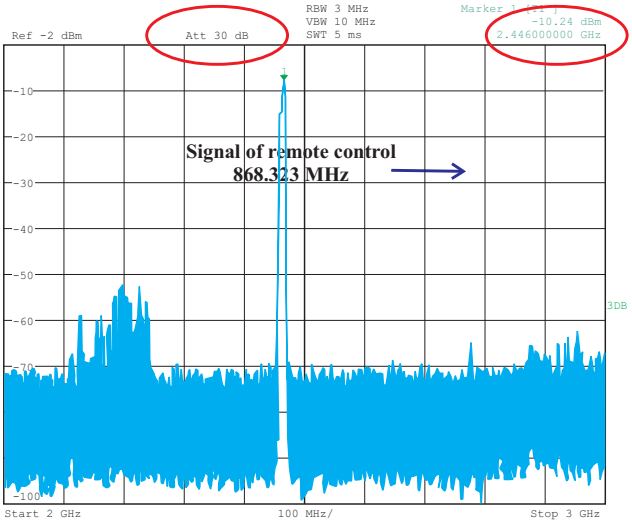

Fig. 24: The result of the measurement of the magnetron.

The full measurement was implemented in 30 seconds (time to turn on the heating of the magnetron) until the temperature of the magnetron was between 90 and 120 °C. The measured power was −10.24 dBm. By using recalculation with the used value of the attenuator, the transmitted power of the magnetron can be calculated and the result (P_o) is 946.237 W. From the values of the energy consumption and the transmitted power, we can verify energy conversion efficient (η) of the used magnetron.

$$\eta = \frac{P_o}{P} = 58\ (\%). \tag{4}$$

4.3. Verifying Functionality of the Interfering Device

The effect of the interference on the wireless band is shown in Fig. 21, where the spectrum of the magnetron overlaps the wireless band.

The goal was, in particular, to test the sensors for their immunity and the interference of UAV commutation.

The interference of the sensors has been accomplished for several meters and the disturbance of UAV at a distance of 1 m. Therefore, for practical use, it is necessary to increase the magnetron power, use a more powerful magnetron, and use a better directional antenna. However, the disadvantages arise that the antenna system of the jamming device increases its size, plus directional antenna is a more complex focus of multiple sensors simultaneously.

5. Conclusion

This article presents a design and implementation of the test version of an interfering mobile device for interference of Wi-Fi signal. The mobile device was implemented using stepper motors controlled with the help of a microcontroller ATmega 16.

The mobile device was designed in two modes. The first mode is controlling of the propulsion of mobile device, e.g. driving forward, backward, turn left and right, and changing speed. The second mode is driving of the rotation of antenna and controlling jammer. The implementation and measurement of the interfering part were shown. The main element of the interfering part is an inverter 12 V/230 V, 60 Hz. The controlling of the inverter was implemented using the circuit control of microcontroller. The measurement of inverter was also mentioned in this article. The result shows that the maximum voltage of the inverter's output is 185 V with a load of 800 Ω, 0.9 A. The measurement of MOT transformer and frequency response of the magnetron was also presented. The test version of the mobile device will be used as a preparation interference of electronic equipment in the Wi-Fi band and measurement electromagnetic compatibility. For future work, we will solve the problem of using battery Li-Po for suppling mobile device and switching inverter with higher frequency for high performance.

Acknowledgment

The work presented in this article has been supported by the Czech Republic Ministry of Defence - University of Defence development program "Pulse High Voltage Converters for Mobile Interference Device with Magnetron" (K-207) and project of K-217.

References

[1] LEUCHTER, J., V. STEKLY and E. BLASCH. Investigation of Avionics Power Switch Loading Versus Aircraft Electromagnetic Compatibility. *IEEE Aerospace and Electronic Systems Magazine*. 2015, vol. 30, iss. 9, pp. 24–34. ISSN 0885-8985. DOI: 10.1109/MAES.2015.140224.

[2] LEUCHTER, J. and P. BAUER. High-Speed generator-converter set for auxiliary power units. In: *30th Digital Avionics System Conference (DASC)*. Seattle: ALR International, 2011, pp. 1–12. ISBN 978-1-61284-798-6. DOI: 10.1109/DASC.2011.6096306.

[3] LEUCHTER, J. and P. BAUER. Review of power electronic concepts of hybrid power source. In: *37th Annual Conference of the IEEE Industrial Electronics Society (IECON 2011)*. Melbourne: IECON, 2011, pp. 3779–3786. ISBN 978-1-61284-971-3. DOI: 10.1109/IECON.2011.6119948.

[4] LEONHARD, W. *Control of electrical drives*. 3rd ed. New York: Springer, 2011. ISBN 3-540-41820-2.

[5] MOHAN, N. *Electric drives: an integrative approach*. Minneapolis: MNPERE, 2000. ISBN 978-0971529250.

[6] BACHA, S., I. MUNTEANU and A. I. BRATCU. *Power electronic converters modelling and control: with case studies*. London: Springer, 2014. ISBN 978-1-4471-5477-8.

[7] LUO, F. L. and H. YE. *Advanced DC/DC converters*. Boca Raton: CRC Press, 2004. ISBN 0-8493-1956-0.

[8] *STANAG 4205 C3: Technical Standards For Single Channel UHF Radio Equipment*. 3rd. Brussels: NATO Standardization Agency, 2005.

[9] Principle-stepper motor. *pohonnatechnika.cz* [online]. 2018. Available at: `http://www.pohonnatechnika.cz/skola/motor/krokovy-motor`.

[10] Stepper motors SX. *MICROCON* [online]. 2018. Available at: `http://www.microcon.cz/PDF082018/motory_SX_092018.pdf`.

[11] REZAC, K. Stepper motors. *Robotika.cz* [online]. 2002. Available at: `https://robotika.cz/articles/steppers/cs`.

[12] Hybrid Stepper Motor: 57mm Series (NEMA 23 size) 1.8 Degree High Torque Type. *LDO MOTORS* [online]. 2018. Available at: `http://ldomotors.com/uploads/product_attachment/path/8/LDO-57STH_Info_Sheet.pdf`.

[13] MTX2-SMA Transmitting micromodule with a battery holder. *FLAJZAR.CZ* [online]. 2018. Available at: `https://eshop.flajzar.cz/gb/elektronics`.

[14] Home of RF and Wireless Vendors and Resources: One Stop For Your RF and Wireless Need. *RF Wireless World* [online]. 2018. Available at: `http://www.rfwireless-world.com/Tutorials`.

[15] LOYKA, S. Electromagnetic interference in wireless communications: behavioral-level simulation approach. In: *IEEE 60th Vehicular Technology Conference*. Los Angeles: IEEE, 2004, pp. 3945–3949. ISBN 0-7803-8521-7. DOI: 10.1109/VETECF.2004.1404817.

[16] CHANGLIN, Z., Z. ZHAN, Q. XUEBING, Y. HONGTAO and Z. WEIDONG. Research on the electromagnetic environment effect on wireless communication systems. In: *8th International Symposium on Antennas, Propagation and EM Theory*. Kunming: IEEE, 2008, pp. 1478–1481. ISBN 978-1-4244-2192-3. DOI: 10.1109/ISAPE.2008.4735510.

[17] YANG, H. Y. D. Analysis of RF radiation interference on wireless communication systems. *IEEE Antennas and Wireless Propagation Letters*. 2003, vol. 2, iss. 1, pp. 126–129. ISSN 1536-1225. DOI: 10.1109/LAWP.2003.816634.

[18] SPIEGEL, S. J., L. BLANKA, H. KUPERSHMIDH, H. B. SINOUR, Y. ABECASIS, A. LEVI and M. HAIUT. Radio frequency interference cancellation in wireless communication systems. In: *IEEE International Conference on Microwaves, Communications, Antennas and Electronic Systems (COMCAS)*. Tel Aviv: IEEE, 2015, pp. 1–4. ISBN 978-1-4799-7473-3. DOI: 10.1109/COMCAS.2015.7360355.

[19] HUY, D. Q., K. ZUBIK, V. STEKLY and J. LEUCHTER. Optimization of the interfering device for use of interference communication UAV. In: *IEEE/AIAA 36th Digital Avionics Systems Conference (DASC)*. St. Petersburg (FL): IEEE, 2017, pp. 1–5. ISBN 978-1-5386-0365-9. DOI: 10.1109/DASC.2017.8101985.

[20] VOLAKIS, J. *Antenna Engineering Handbook*. 4th ed. New York: McGraw-Hill, 2007. ISBN 978-0071475747.

[21] Effective Isotropic Radiated Power (EIRP). *Antenna-Theory.com* [online]. 2018. Available at: `http://www.antenna-theory.com/definitions/eirp.php`.

About Authors

Jan LEUTCHTER was born in Pardubice, the Czech Republic. He received his M.Sc. from University of Defence in 1999. His research interests include Power electronics and EMC. His main areas of expertise are power processing, power quality and power sources. The focus of his current research is on EMC test of the aircraft electrical systems.

Huy DONG QUANG was born in Thai Binh, the Vietnam. He received his M.Sc. from University of Defence in 2015. His research interests include Radio technology. The focus of his current research is on EMC test of the electrical systems.